Anti- and Prooxidant Properties of Carotenoids

Hans-Dieter Martin*, Claudia Jäger, Christoph Ruck, and Marcus Schmidt

Düsseldorf, Institute of Organic Chemistry and Macromolecular Chemistry, University

Robin Walsh

Reading/UK, Department of Chemistry, University

Joachim Paust

Ludwigshafen, BASF AG

Received Februar 8th, 1999

Dedicated to Professor Fritz Vögtle on the Occasion of his 60th Birthday

Keywords: Autoxidation, Carotenoids, Oxygen, Antioxidant, Prooxidant

Abstract. Carotenoids can be effective singlet oxygen quenchers and inhibit free-radical induced lipid peroxidation. A remarkable property of β-carotene (**1a**) is the change from an antioxidant to a prooxidant depending on oxygen pressure and concentration. In the present study a considerable number of carotenoids (**1a**, **2c**, **2d**, **2e**, **3a**, **4a**, **5a**, **6a**, **7a**, **8a**, **8h**, **8i**, **8j**, **9f**, **10a**, **11a**, **12g**) was investigated using two independent approaches: 1. Comparison of their effects on inhibition of the free-radical oxidation of methyl linoleate, and 2. The direct study of the effect of oxygen partial pressure upon their rates of oxidation. It is shown that some carotenoids (**7a**, **8a**) are even more effective than the well-known compounds β-carotene (**1a**) and astaxanthin (**5a**) and are powerful antioxidants without any prooxidative property. Different carotenoids display different behaviour depending on chain length and end groups. The influence of these functional groups on the antioxidative reactivity is discussed.

Carotenoids are widely distributed in nature where they play an important role in cell protection [1]. Oxygen species including $^1O_2$, $^3O_2$ and $O_2^{\cdot -}$ are capable to damage lipid membranes as well as DNA, and become the cause of mutation of cell material. Carotenoids can play the role of versatile antioxidants because they are effective biological quenchers as well as radical chain breaking agents [2]. Many studies including *in vitro*, *in vivo* and epidemiological tests were carried out to investigate these properties of carotenoids [3–5]. β-Carotene (**1a**), as the best known carotenoid compound, shows the remarkable effect of changing its antioxidant to a prooxidant behaviour at high concentrations of β-carotene and in the presence of high oxygen partial pressures [2]. Since epidemiological studies can show contradictory and confounding results [3–5], a more thorough inspection of the anti- and prooxidant functions of carotenoids is needed. Carotenoids with antioxidative properties better than β-carotene (**1a**), like astaxanthin (**5a**), have attracted special interest [6a,c].

In this study we present an approach to a better understanding of these anti- and prooxidant properties of carotenoids and describe carotenoids, both natural and synthetic, with sole antioxidant efficiency approaching that of α-tocopherol.

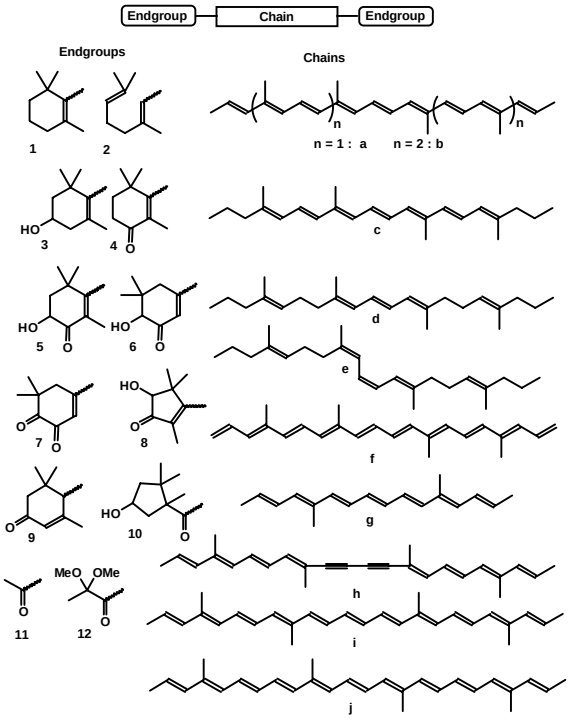

Scheme 1 Structures of all investigated carotenoid compounds **1**– **12**

  1436-9966/99/3410X-302 $ 17.50 + .50/0

Synthesis, characterization, and properties of the carotenoids are described in several published articles [7–9], all other compounds will be introduced in this publication (see Experimental). β-Carotene (**1a**), canthaxanthin (**4a**), zeaxanthin (**3a**), astaxanthin (**5a**), lycopene (**2a**), tetrahydrolycopene (**2c**), 13-*cis*-Phytoene (**2e**) and all-*trans*-Phytoene (**2d**) were provided by BASF AG. Rhodoxanthin (**9f**) was generously supplied by Dr. A. Rüttimann, Hoffmann La Roche, methyl linoleate (99%) was obtained from Aldrich, cumene from Merck, *dl*-α-tocopherol (98%) (**14**) from Fluka and 2,2'-azobis(2,4-dimethylvaleronitril) (AMVN) from Wako. All chemicals were stored at –20 °C. Pure solvents (*p.a.*) were used as received.

Method 1

Experimental Parameters

This method (similar to that described in ref. [6a]) made use of radical induced formation of methyl linoleate hydroperoxides and monitored the increase *via* HPLC-DAD-detection at 235 nm. Carotenoids were monitored at their corresponding λ_{max} wavelengths. The reaction was carried out in a mixture of *n*-hexane, isopropanol and chloroform (volume ratio 6:5:2, 6.5ml sample volume) at 37 °C followed by HPLC-analysis (solvent: *n*-hexane/isopropanol = 99:1; follow rate 2.0 ml/min, column: YMC SIL-ASP,150×6 mm, S-5 µm, 60*A* [6a]) in 20–30 min intervals (diode array UV-Vis: HP 1 040m Serie II; pumping and injection system: HP 1 050).

β-Carotene (**1a**), astaxanthin (**5a**), actinioerythrol (**8a**) as well as other carotenoids were used at concentrations of 7.7×10^{-4} M. The concentration of the initiator AMVN was 7.7×10^{-3} M and of methyl linoleate was 7.7×10^{-2} M. Different from ref. [6a] antioxidants (carotenoids, *dl*-α-tocopherol) were dissolved in chloroform instead of tetrahydrofuran, because of the low solubility of the compounds (especially actinioerythrol). Reference measurements showed that change of solvent does not affect the results.

Reaction Vessel

To get reproducible results, the vessel has to meet the following requirements: Tab. 1 shows that the reaction converts larger amounts of methyl linoleate (ca. 6% after 5 hours) into the corresponding peroxides. The antioxidants, especially the carotenoids, consume amounts of oxygen 5 to 6 times higher than their concentration [7]. To get results which do not depend on the amount of oxygen, there must be a large excess oxygen available in the reaction vessel. A closed system avoids loss of solvent (high vapor pressures of solvents at 37 °C). This loss would result in erroneously increased amounts of peroxides. The internal equilibrium pressure after 10–20 minutes is ca. 1 250 mbar.

Analysis

Reference measurements showed that the original content of peroxide (0.1–0.5%) does not affect the results. Data points obtained were linearly interpolated for 30 minutes intervals. Other interpolation methods lead to similar results. Each graph represents the average of eight 6 hour measurements.

Method 2

This method (related to the method of Burton and Ingold [2]) was carried out using a pressure transducer (MKS Baratron 223B) to monitor the uptake of oxygen pressure in a sealed reaction vessel and with it the consumption of oxygen during the radical induced oxidation (AMVN, 4.5×10^{-2} M) at 30 °C in chlorobenzene. The system was capable of being filled with different mixtures of O_2 and N_2 containing 20, 200 and 1 013 mbar (15, 150 and 760 Torr) of oxygen partial pressure. The samples were injected into the reaction vessel *via* a septum.

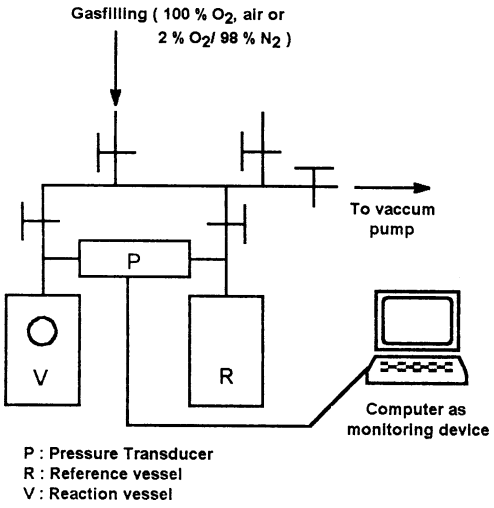

Fig. 1 Reaction vessel for studying pressure dependence

The following experiments were performed: the radical induced autoxidation of **1a** and **5a** and protective properties of carotinoids – compounds **1a**, **1b**, **2a**, **2c**, **2d**, **2e**, **3a**, **4a**, **5a**, **6a** and **8a** – against the oxidation of cumene (3.57 M) were investigated at concentrations of 5×10^{-5} M, 1×10^{-4} M, 5×10^{-4} M, 1×10^{-3} M and 5×10^{-3} M.

Results and Discussion

Method 1: Oxidation of Methyl Linoleate

The following plot displays the antioxidant activity of some investigated carotenoids. Quantitative compari-

Table 1 Peroxide formation of pure methyl linoleate (No. 1) and in the presence of antioxidants (No. 2 – 19). 50 % Astaxanthin means: the standard concentration 7.7×10^{-4} M is reduced by 50%.

No.	Compound name	% Peroxide
1	Methyl linoleate	6.11
2	Tetrahydrolycopene **2c**	6.10
3	13-*cis*-Phytoene **2e**	4.73
4	trans-Phytoene **2d**	4.22
5	Acyloin **8h**	2.67
6	Acyloin **8i**	2.03
7	β-Carotene **1a**	2.21
8	Diketone **12g**	2.04
9	50% Astaxanthin **5a**	1.52
10	Capsorubin **10a**	1.04
11	Acyloin **8j**	0.70
12	Isonorastaxanthin **6a**	0.65
13	Rhodoxanthin **9f**	0.64
14	Astaxanthin **5a**	0.60
15	Diketone **11a**	0.54
16	70% Actinioerythrol **8a**	0.51
17	Isonorastacene **7a**	0.47
18	Actinioerythrol **8a**	0.43
19	α-Tocopherol	0.14

son can be achieved by choosing the amount of peroxide after 5 hours as parameter to describe the activity.

The results of Fig.2 show that the amount of peroxide in the uninhibited autoxidation of methyl linoleate is 6.1%. This is much more than recently described (ca. 0.8%). β-Carotene and astaxanthin drop the peroxide formation to 2.2%/0.6% (ref. [6a]: ca.0.5%/0.25%). The relative antioxidant abilities of β-carotene and astaxanthin turn therefore out to be stronger than suggested [6a]. It seems that astaxanthin has been underestimated..

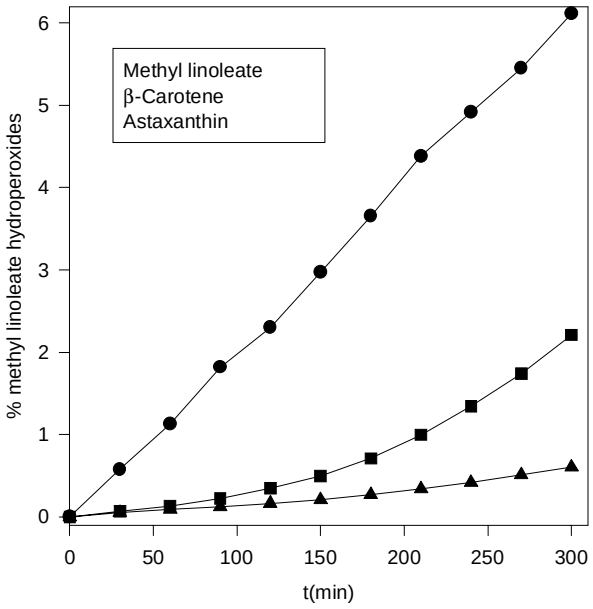

Fig. 2 Comparison of methyl linoleate ●, β-carotene ■ and astaxanthin ▲. % of methyl linoleate hydroperoxide is the amount of methyl linoleate converted to hydroperoxide. Experimental errors are ± 5%

Figure 2 reflects the antioxidative effect of β-carotene and astaxanthin on the uninhibited autoxidation of methyl linoleate. The diketone capsorubin (**10a**) is a stronger inhibitor than β-carotene although the conjugated π-system has the same number of double bonds. The main reason is that the polyene chain of capsorubin is more related to astaxanthin than to β-carotene because of its terminating carbonyl groups. Carbonyl stabilization is one of the important factors in stabilizing radical intermediates of the chain reaction and is impeding further autoxidation of methyl linoleate. This idea is supported by the antioxidative strength of diketone **11a** containing the chromophoric system of capsorubin (**10a**) [10]. Surprisingly, the antioxidant efficiency of **11a** is slightly better than that of astaxanthin. Introduction of larger end groups can reduce antioxidant activity, either because of sterical or electronic reasons. Another interesting and important structural factor is the position and number of methyl groups in the polyene chain, cf. acyloins **8i** and **8j**.

The effects of additional oxo groups and ring contraction are remarkable: the results show that astaxanthin has only 60–70% of the antioxidant activity of actinioerythrol (**8a**) and isonorastacene (**7a**)!

Comparing isonorastaxanthin (**6a**) and isonorastacene (**7a**) it can be seen that the high antioxidant activity of isonorastacene (**7a**) is due to an increase in conjugated carbonyl groups resulting in excessive radical stabilization.

A slight increase in conjugation length does not show any significant influence on the antioxidant ability. The value for rhodoxanthin (**9f**) is within experimental error the same as for astaxanthin.

Terahydrolycopene (**2c**) has practically no influence on the inhibition of the autoxidation of methyl linoleate, although the chain contains seven conjugated double bonds. On the other hand the investigated phytoenes show a stronger antioxidant activity , in spite of the small π-system (three conjugated double bonds).

Method 2: The Effect of Oxygen Partial Pressure

Previous results show [2], that oxygen partial pressure has an important influence on these reactions. In case of β-carotene the antioxidative effect was converted into a prooxidative property for high carotenoid concentrations and high oxygen partial pressures. The following study investigates several carotenoids using the radical induced oxidation of cumene as model system.

Figure 3 shows four selected graphs. Curve A reflects the oxidation without any carotenoid. The addition of β-carotene in low concentrations (5×10^{-5} M and 5×10^{-4} M) slows down the uptake of pressure and the consumption of oxygen (curve B and C).The additive acts

as an antioxidant. But using a higher dose of the carotenoid (curve D/5×10^{-3} M) the reaction speeds up again, consuming more oxygen and showing now the prooxidative property of the supplement.

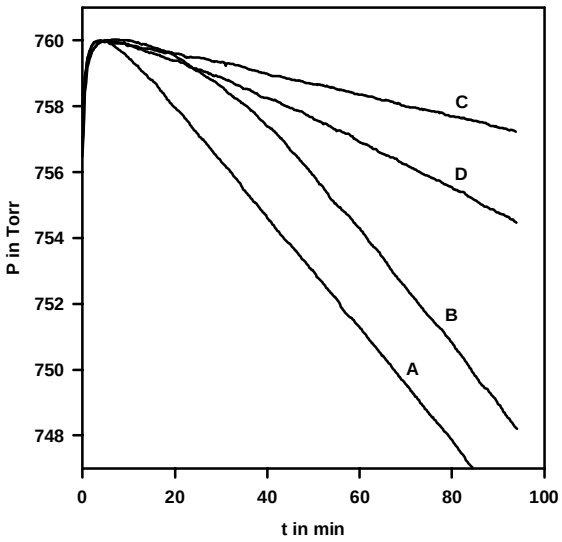

Fig. 3 Radical induced oxidation of cumene without (A) and with added (B, C, D, see text) β-carotene

The investigated carotenoids can be divided into three classes. The first group contains molecules with very little antioxidative capability (**2c**, **2d**, **2e**), and these are therefore not of interest here. The second class comprises compounds with good antioxidative but also prooxidative properties (β-carotene (**1a**), see Figure 4, **1b**, **2a, 3a**).

The third class consists of carotenoids which react as strong antioxidants and without any prooxidative nature (**4a**, **5a**, **6a**, **8a**). All of them contain conjugated oxo-functions within their end groups. The results for astaxathin as model compound are presented in Figure 5.

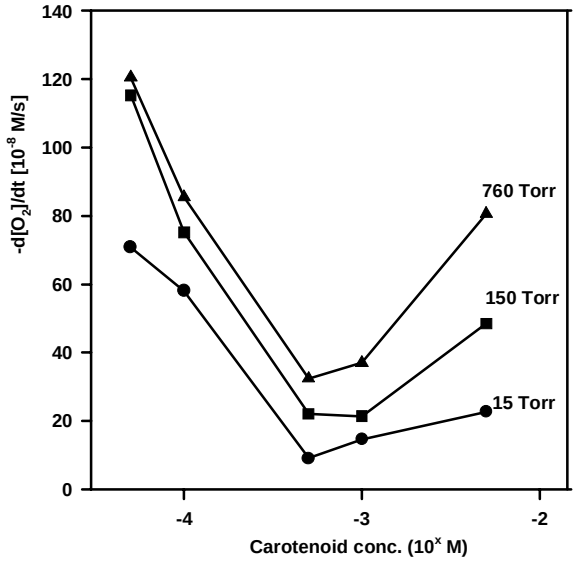

Fig. 4 Effect of partial pressure of oxygen and of β-carotene concentration on the rate of oxidation of cumene

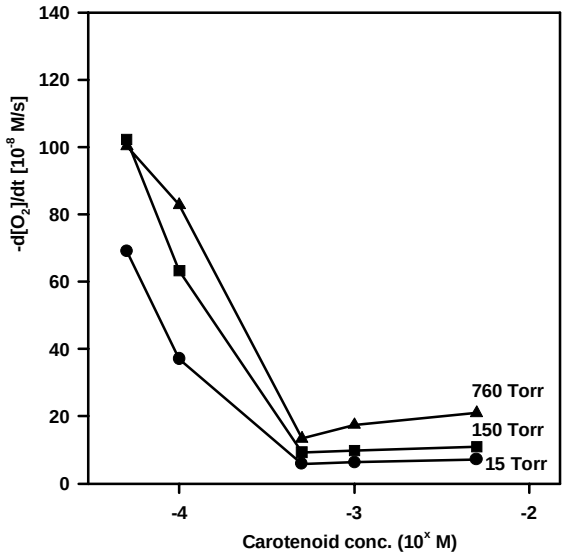

Fig. 5 Effect of partial pressure of oxygen and of astaxanthin concentration on the rate of oxidation of cumene

In the concentration range between 5×10^{-5} M and 5×10^{-4} M the two carotenoids β-carotene and astaxanthin display similar behaviour. Both compounds start by behaving as an antioxidant slowing down the oxidation rate and reaching their maximal antioxidative activity at about 5×10^{-4} M. At this point astaxanthin shows its higher antioxidative capability, especially in the presence of larger quantities of oxygen.

However, for molarities higher than 5×10^{-4} M β-carotene turns into a prooxidant for all tested oxygen partial pressures. In sharp contrast, astaxanthin does not show

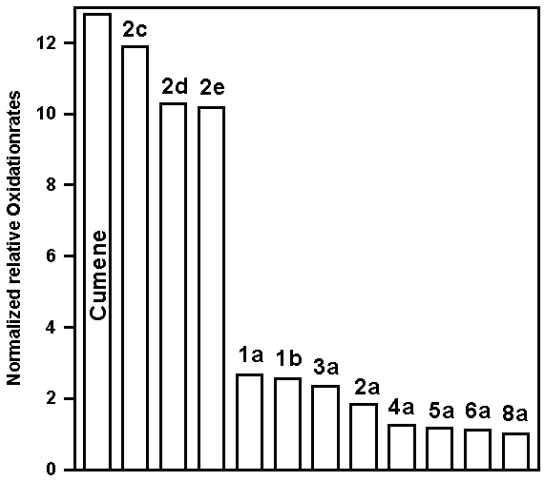

Fig. 6 Normalized (with respect to actinioerythrol (**8a**) = 1) rates of oxidation at $p(O_2)$ = 150 Torr

this behaviour. Only a slight increase of the oxidation rate is observed for highest oxygen partial pressures, quite different from the changes recorded for β-carotene. For pressures of oxygen < 760 Torr invariant rates of oxygen consumption demonstrate a zero increase of oxidation.

To compare these results with those of method 1 the relative rates of oxidation were normalized to the powerful carotenoid-antioxidant actinioerythrol (**8a**) and extrapolated to the concentration of 7.7×10^{-4} M (Figure 6). In both methods, the oxo-compounds, *e.g.* **5a** or **8a**, behave as best antioxidants. The polyenes **2c**, **2d** and **2e**, however, are the weakest inhibitors in this study. The non-oxo xanthophylls, like **3a**, are found in between. Both results underline that the influence of the end groups as well as of the polyene chain is important for the antioxidative strategy.

Further studies are made by investigating the radical induced autoxidation of the two model compounds β-carotene and astaxanthin. In general the reaction rate increases with increasing concentration of carotenoid and increasing partial pressure of oxygen. But the oxidation of astaxanthin is much slower for all oxygen partial pressures than the rate of β-carotene.

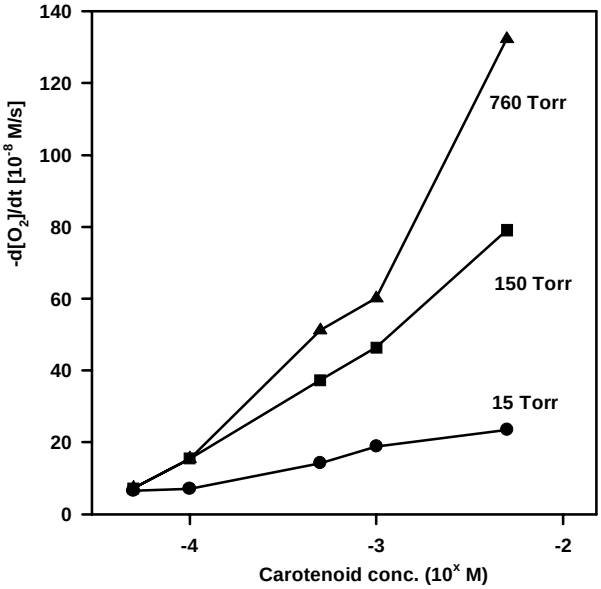

Fig. 7 Dependence of the rate of oxygen consumption on carotenoid concentrations and partial pressures of oxygen for β-carotene

To find a model that is able to explain the pressure dependence we have started to simulate the autoxidation of β-carotene (using the program Acuchem). In this simulation the following reaction sequence is used (see scheme 2), that is not only capable to explain the formation of the various products (epoxides, carbonyl compounds [1,4,11]), but also to obtain an already quite reasonable fit to our experimental results (as an example see Figure 8). The chain reaction (Car·) provides for the efficient consumption of carotenoids in case of class I and class II carotenoids.

CarH	+	ROO•	→	Car•	+	ROOH
Car•	+	O_2	→	Car-O_2•		
Car-O_2•	+	CarH	→	Car-O_2-CarH•		
Car-O_2-CarH•			→	Car-O•	+	Epoxide
Car-O•	+	CarH	→	Car-O-CarH•		
Car-O-CarH•	+	O_2	→	Car-O-CarH-O_2•		
Car-O-CarH-O_2•	+	CarH	→	Car-O-CarH-O_2-CarH•		
Car-O-CarH-O_2-CarH•			→	Car-O-CarH-O•	+	Epoxide
Car-O-CarH-O•			→	Car•	+	2 Carbonyls

Scheme 2 Prosed reaction scheme for the mechanism of β-Carotene (**1a**) autoxidation that uses radical addition, fragmentation and hydrogen abstraction reactions and is able to fit the experimental results

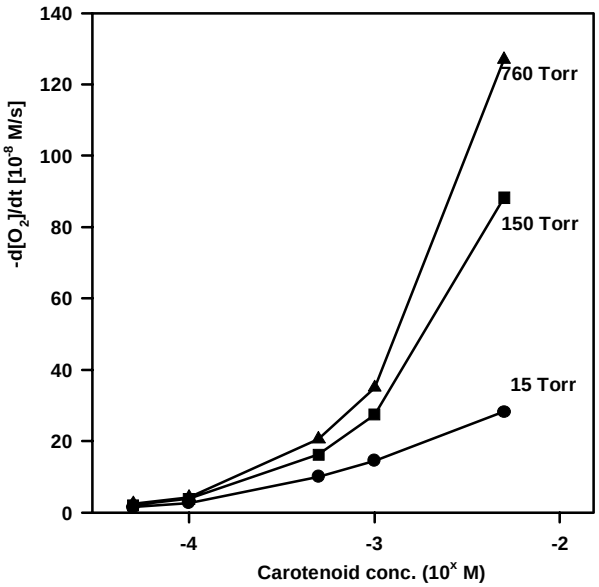

Fig. 8 Simulated oxidation rates of β-carotene for different oxygen partial pressure and different carotenoid concentrations are shown. These simulations may be compared with the experimental results of Figure 7

Conclusion

These results lead to the suggestion that the different chemical anti- and prooxidant behaviour of the carotenoids is caused by the different structure of their end groups, their chain length (minor importance) and the number and position of methyl groups. The following proposals are made: β-carotene is able to react as a hydrocarbon with active allylic hydrogen atoms that can be removed by radicals. On the other hand β-carotene can also bind to peroxyl radicals. Both processes combine to produce chain reactions (scheme 2) with the concomitant formation of epoxides and carbonyl compounds. Thus, it is possible to develop a sequence of radical abstraction and oxygen addition reactions as well

as cleavage reactions resulting in a radical chain reaction.

In contrast astaxanthin does not seem to undergo these pathways or does it much slower. The proposal, that the oxo function is capable to resonance-stabilize carbon-centered radicals might explain the powerful antioxidative properties of all class III carotenoids without prooxidative contributions, particularly the remarkable efficacy of isonorastacene (**7a**) and actinioerythrol (**8a**).

This work was supported by BASF AG and the Fonds der Chemischen Industrie.

Experimental

Melting points (uncorrected) were determined on Thermovar, Fa. Reichert, Wien/Österreich. – Gas chromatography: Hewlett-Packard 5890 A, SE 30, Injector temperature 230 °C, 16 °C/min from 80 °C to 230 °C. – TLC: Merck DC-Folie, silicagel 60, Fluor.indic. F_{254} (0.2 mm). – CC: silicagel 60, 230–400 mesh, Merck. – ^{1}H NMR spectra: 300 MHz Varian VXR 300. – ^{13}C NMR spectra, – ^{31}P NMR spectra: 75 MHz Varian VXR 300, 200 MHz Bruker AM 200. – IR spectra: Perkin-Elmer 710 B. – UV/Vis spectra: Zeiss DMR 21, M4 Q III. – Mass spectra: Varian MAT/CH-5, Varian MAT 311 A, IE 70 eV. – GC/MS: Hewlett–Packard 5890 10m capillar column HP OV-1-FS, Hewlett–Packard 5970, IE 70 eV. – High–resolution MS: Finnigan MAT 95, IE 70 eV.

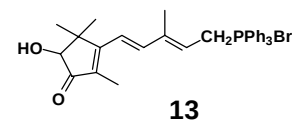

13

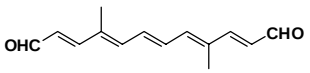

14

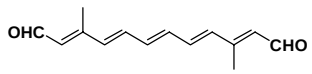

15

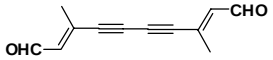

16

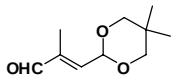

17

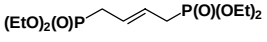

18

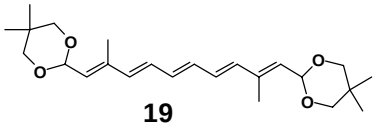

19

1,22-Bis-(4-hydroxy-2,5,5-trimethyl-3-oxo-1-cyclopentenyl)-3,9,14,20-tetramethyl-docosa-undeca-1,3,5,7,9,11,13,15,17,19,21-en (**8j**)

Phosphoniumsalt **13** (3.50 g, 6.2 mmol) [12] is dissolved in 100 ml 1,2-epoxybutane under nitrogen. After addition of 0.34 g (1.5 mmol) C_{14}-dialdehyde **14** [13] the mixture is heated to reflux for 24h. The solution is poured on saturated ammonium chloride solution and extracted four times with dichloromethane. The organic phases are dried over sodium sulfate. After evaporation the crude product is dissolved in a small amount of dichloromethane, and 50 ml methanol are added. After evaporation of dichloromethane the product crystallizes over night at –18 °C. The precipitate is purified *via* chromatography on silica gel using diethyl ether. – Yield 0.12 g (12%), *m.p.* 205 °C. – ^{1}H NMR ($CDCl_3$): δ/ppm = 1.18 (s, 6H, 18/19H), 1.41 (s, 6H, 19/18H), 1.91 (s, 6H, 20H), 1.97 (s, 6H, 22H), 2.01 (s, 6H, 21H), 2.69 (d, J = 3.0 Hz, 2H, OH), 3.94 (d, J = 2.5 Hz, 2H, 3H), 6.35 (d, J = 9.9 Hz, 2H, 14H), 6.42 (d, J = 15.7 Hz, 2H, 7–H), 6.44 (d, J = 9.4 Hz, 2H, 10H), 6.67 (d, J = 10.9 Hz, 2H, 16H), 6.53 (m, 2H, 12H), 6.64 (m, 2H, 13H), 6.66 (m, 2H, 11H), 6.68 (m, 2H, 17H), 6.95 (d, J = 16.2 Hz, 2H, 8H). – ^{13}C NMR ($CDCl_3$): δ/ppm = 9.50 (20-C), 12.28 (21-C), 12.72 (22-C), 23.96 (18/19-C), 25.36 (19/18-C), 45.21 (1-C), 81.68 (3-C), 119.41 (7-C), 128.92 (12-C), 129.10 (11-C), 130.78 (5-C), 130.86 (16-C), 134.05 (15-C), 135.19 (9-C), 136.69 (17-C), 137.11 (14-C), 137.22 (10-C), 139.36 (13-C), 143.84 (8-C), 169.71 (6-C), 206.65 (4-C). – UV/Vis ($CHCl_3$): λ_{max}/nm (lg ε) = 500 sh, 533 (4.98), 570 sh. – MS (EI) *m/z* (%): 620 (12) M^+, 307 (11), 176 (11), 154 (100), 137 (60), 136 (89), 107 (32), 91 (22), 98 (36), 51 (24). – High resolution MS (70 eV).
$C_{42}H_{52}O_4$ Calcd.: 620.38655, Found: 620.38695 ± 0.00362.

1,22-Bis-(4-hydroxy-2,5,5-trimethyl-3-oxo-1-cyclopentenyl)-3,8,15,20-tetramethyl-docosa-undeca-1,3,5,7,9,11,13,15,17,19,2-en (**8i**)

Analogous to **8j** 3.50 g (6.2 mmol) phosphoniumsalt **13** are treated with 0.34 g (1.5 mmol) C_{14}-dialdehyde **15** [13]. – Yield 0.13 g (13%), *m.p.* 210 °C. – ^{1}H NMR ($CDCl_3$): δ/ppm = 1.18 (s, 6H, 18/19H), 1.41 (s, 6H, 19/18H), 1.91 (s, 6H, 20H), 1.99 (s,6H, 21H), 2.01 (s, 6H, 22H), 2.66 (d, 2H, J = 3.9 Hz, OH), 3.92 (d, 2H, J = 3.0 Hz, 3H), 6.39 (d, 2H, J = 12.4 Hz, 15H), 6.46 (d, 2H, J = 16.4 Hz, 7H), 6.47 (d, 2H, J = 11.0 Hz, 10H), 6.67 (m, 2H, 12H), 6.69 (d, 2H, J = 10.8 Hz, 13H), 6.71 (m, 2H, 16H), 6.73 (m, 2H, 11H), 6.78 (m, 2H, 17H), 6.96 (d, 2H, J = 16.0 Hz, 8H). – ^{13}C NMR ($CDCl_3$): δ/ppm = 9.5 (20-C), 12.31 (21-C), 12.78 (22-C), 23.96 (18/19-C), 25.36 (19/18-C), 45.20 (1-C), 81.68 (3-C), 119.50 (7-C), 129.48 (11-C), 130.01 (12-C), 130.88 (5-C), 130.91 (16-C), 132.66 (17-C), 134.19 (15-C), 135.38 (9-C), 137.48 (14-C), 137.56 (10-C), 138.23 (13-C), 143.81 (8-C), 169.66 (6-C), 206.62 (4-C).– UV/Vis ($CHCl_3$): λ_{max}/nm (lg ε) = 500 sh, 531 (4.97), 560 sh. – MS (EI) *m/z* (%): 620 (4) M^+, 307 (11), 154 (100), 136 (80), 77 (37), 51 (22).

1,20-Bis-(4-hydroxy-2,5,5-trimethyl-3-oxo-1-cyclopentenyl)-3,8,13,18-tetramethyl-eicosa-oct-1,3,5,7,13,15,17,19en-9,11-diin (**8h**)

Analogous to **8j** 3.50 g (6.2 mmol) phosphoniumsalt **13** are treated with 0.30 g (1.5 mmol) C_{14}-diindialdehyde **16** [13]. – Yield 0.20 g (21%), *m.p.* 196–198 °C. – ^{1}H NMR ($CDCl_3$): δ/ppm = 1.18 (s, 6H, 17/18H), 1.41 (s, 6H, 18/17H), 1.91 (s, 6H, 19H), 1.99 (s, 6H, 20H), 2.02 (s, 6H, 21H), 2.71 (d, 2H, J = 3.8 Hz, OH), 3.94 (s, 2H, 3H), 6.42 (m, 2H, 11H), 6.44 (d, 2H, J = 16.4 Hz, 7H), 6.65 (m, 2H, 12H), 6.68 (d, 2H, J = 10.9 Hz, 13H), 6.69 (d, 2H, J = 10.3 Hz, 10H), 6.94 (d, 2H, J = 16.1 Hz, 8H). – ^{13}C NMR ($CDCl_3$): δ/ppm = 9.49 (19-C), 12.41 (20-C), 17.35 (21-C), 23.94 (17/18-C), 25.31 (18/17-

C), 45.20 (1-C), 76.75 (1-C), 77.21 (15-C), 81.66 (3-C), 87.96 (14-C), 87.97 (15-C), 119.29 (9-C), 119.30 (16-C), 120.42 (7-C), 131.04 (11-C), 131.41 (12-C), 136.44 (13-C), 137.31 (5-C), 138.71 (10-C), 143.40 (6-C), 169.40 (6-C), 206.75 (4-C). – UV/Vis ($CHCl_3$): λ_{max} (lg ε) = 420 sh, 467 (4.86), 505 sh. – MS (EI) *m/z* (%): 590 (5) [M^+], 152 (21), 139 (26), 124 (24), 123 (29), 121 (14), 119 (12), 109 (42), 81 (71), 79 (33), 77 (31), 67 (41), 55 (52), 43 (83), 41 (100), 39 (67). – High resolution MS (70 eV).
$C_{40}H_{46}O_4Na$ Calcd.: 613.32937, Found: 613.33411 ± 0.00323.

7,14-Dimethyl-2,2,19,19-tetramethoxyeicosa-hept- 4,6,8,10, 12,14,16-en-3,18-dion (**12g**)

In a 250 ml three-necked flask with condenser and nitrogen-interface 0.5 g (2.3 mmol) C_{14}-dialdehyde **15** and 0.65 g (11.5 mmol) potassium hydroxide are dissolved in 65 ml dry methanol at 70 °C. Under nitrogen 1.5 g (11.5 mmol) 3,3-dimethoxybutan-2-on in 50 ml dry methanol are added dropwise at 70 °C. The mixture is stirred for 6 h at 70 °C and neutralized with acetic acid. After addition of 150 ml of water the organic phase is extracted four times with 100 ml of chloroform. The organic layers are dried over sodium sulfate. The residue is purified *via* column chromatography (dichloromethane/diethyl ether 10:1, R_f = 0.27). After addition of ethanol the product crystallizes at 0 °C. – Yield 0.21 g (20%), *m.p.* 137 °C. – ^{1}H NMR ($CDCl_3$): δ/ppm = 1.42 (s, 6H, 1H), 2.07 (s, 6H, 13H), 3.27 (s, 12H, 11H, 12H), 6.32 (d, J = 12.1 Hz, 2H, 6H), 6.42 (d, J = 14.8 Hz, 2H, 8H), 6.50 (m, 2H, 9H), 6.56 (m, 2H, 10H), 6.72 (d, J = 14.9 Hz, 2H, 4H), 7.82 (dd, J = 12.1 Hz, 14.9 Hz, 2H, 5H). – ^{13}C NMR ($CDCl_3$): δ/ppm = 31.20 (13-C), 20.20 (1-C), 49.79 (11-C, 12-C), 102.32 (2-C), 123.76 (4-C), 130.63 (6-C), 132.54 (10-C), 135.29 (9-C), 137.67 (8-C), 140.32 (5-C), 146.19 (7-C), 197.12 (3-C). – UV/Vis ($CHCl_3$): λ_{max} (lg ε) = 449 (5.23), 475 (5.21). – MS (EI) *m/z* (%): 444 (20) M^+, 413 (5), 280 (6), 149 (26), 89 (100), 43 (69), 32 (23).

$C_{26}H_{36}O_6$	Calcd.:	C 70.18	H 8.10
(444.6)	Found:	C 69.87	H 8.17.

1,10-Bis-(5,5-dimethyl-1,3-dioxan-2-yl)-2,9-dimethyl-deca-penta-1,3,5,7,9-en (**19**)

In a 500 ml two-necked flask 7.8 g (120.0 mmol) sodium hydride are suspended in 200 ml dry tetrahydrofuran under nitrogen. 19.2 g (58.5 mmol) phosphonate **18** in 100 ml dry tetrahydrofuran are added dropwise at room temperature. After hydrogen evolution 27.6 g (150.0 mmol) aldehyde **17** in 100 ml dry tetrahydrofuran are added at room temperature. After stirring for 48 h diethyl ether is added, and the product precipitates as a bright yellow solid which is filtered and dried *in vacuo*.
Yield 11.0 g (47%), *m.p.* 199 °C. – ^{1}H NMR ($CDCl_3$): δ/ppm = 0.74 (s, 6H, C–CH_3), 1.22 (s, 6H, C–CH_3), 1.86 d, J = 1.1 Hz, 6H, 7H), 3.52 (d, J = 10.6 Hz, 4H, O–CH_A), 3.65 (d, J = 11.3 Hz, 4H, O–CH_B), 5.19 (d, J = 6.3 Hz, 2H, 2H), 5.55 (d, J = 6.1 Hz, 2H, 4H), 6.33 (m, 2H, 5H), 6.37 (m, 2H, 6H), 6.38 (d, J = 6.6 Hz, 2H, 1H). – MS (EI) *m/z* (%): 388 (10) [M^+], 115 (24), 72 (28), 56 (100), 45 (48), 43 (48).

3,10-Dimethyl-dodeca-penta-2,4,6,8,10-en-1,12-dial (**15**)

Removal of the protective group is achieved by dissolving 11.0 g (28.3 mmol) of **19** in 300ml acetone and 100 ml 1*N* sulphuric acid. After stirring for 2 h at room temperature the yellow precipitate is filtered and dried *in vacuo*. – Yield 5.8 g (95%), *m.p.* 190 °C. – ^{1}H NMR ($CDCl_3$): δ/ppm = 2.31 (s, 6H, 7H), 6.01 (d, J = 8.0 Hz, 2H, 2H), 6.47(d, J = 15.3 Hz, 2H, 4H), 6.58 (m, 2H, 6H), 6.82 (qd, J = 7.4 Hz; 3.0 Hz, 2H, 5H), 10.13 (d, J = 8.0 Hz, 2H, 1H). – ^{13}C NMR ($CDCl_3$): δ/ppm = 12.98 (7-C), 130.42 (4-C), 135.31 (6-C), 136.26 (5-C), 137.49 (2-C), 153.57 (3-C), 191.12 (1-C). – UV/Vis ($CHCl_3$): λ_{max} (lg ε) = 384 (4.79), 405 (4.77). – MS (EI) *m/z* (%): 216 (55) [M^+], 134 (100), 121 (58), 115 (70), 95 (77), 91 (45), 69 (68), 41 (62).

$C_{14}H_{16}O_2$	Calcd.:	C 77.75	H 7.46
(216.3)	Found:	C 77.69	H 7.53.

References

[1] N. I. Krinsky, Free Rad. Biol. Med.**1989**, *7*, 617
[2] G. W. Burton, K. U. Ingold, Science **1984**, *224*, 569
[3] a) J. A. Olson, N. I. Krinsky, FASEB J. **1995**, *9*, 1547; b) G. Britton, FASEB J. **1995**, *9*, 1551
[4] S. T. Mayne, FASEB J. **1996**, *10*, 690
[5] a) R. Edge, D. J. McGarvey, T. G. Truscott, J. Photochem. Photobiol. B **1997**, *41*, 189; b) D. P. T. Steenvoorden, G. M. J. Beijersbergen van Henegouwen, J. Photochem. Photobiol. B **1997**, *41*, 1
[6] a) J. Terao, Lipids **1989**, *24*, 659; b) H. Tsuchihashi, M. Kigoshi, M. Iwatsuki, E. Niki, Arch. Biochem. Biophys. **1995**, *323*, 137; c) W. Miki, Pure and Appl. Chem. **1991**, *63*, 141; d) P. Palozza, G. Calviello, G. M. Bartoli, Free Rad. Biol. Med. **1995**, *19*, 887; e) P. Palozza, C. Luberto, G. Calviello, P. Ricci, G.M. Bartoli, Free Rad. Biol. Med. **1997,** *22*, 1065
[7] R. C. Mordi, J. C. Walton, G. W. Burton, L. Hughes, K. U. Ingold, D. A. Lindsay, D. J. Moffatt, Tetrahedron **1993**, *49*, 911
[8] D. Baltschun, S. Beutner, K. Briviba, H.D. Martin, J. Paust, M. Peters, S. Röver, H. Sies, W. Stahl, A. Steigel, F. Stenhorst, Liebigs Ann./Recueil **1997**, 1887
[9] G. Broszeit, F. Diepenbrock, O. Gräf, D. Hecht, J. Heinze, H.D. Martin, B. Mayer, K. Schaper, A. Smie, H.H. Streblow, Liebigs. Ann./Recueil **1997**, 2205
[10] C. K. Warren, B. C. L. Weedon, J. Chem. Soc. **1958**, 3972
[11] D. C. Liebler, T. A. Kennedy; Meth. Enzymol., **1992**, *213*, 472
[12] F. Stenhorst, Dissertation, Universität Düsseldorf 1996
[13] a) H. Mayer, M. Montavon, R. Rüegg, O. Isler, Helv. Chim. Acta **1967**, *50*, 1606; H. Ippendorf, Dissertation, Universität Düsseldorf 1992

Address for correspondence:
Prof. Dr. H.-D. Martin
Heinrich-Heine-Universität Düsseldorf
Institut für Organische Chemie und Makromolekulre Chemie
Universitätsstr. 1
D-40225 Düsseldorf
Fax: Internat. code (0) 211-81-14324
e-mail: martin@uni-duesseldorf.de